EJN fens EUROPEAN JOURNAL OF NEUROSCIENCE

European Journal of Neuroscience, Vol. 35, pp. 353–365, 2012 doi:10.1111/j.1460-9568.2011.07958.x

MOLECULAR AND DEVELOPMENTAL NEUROSCIENCE

Cysteine- and glycine-rich protein 1a is involved in spinal cord regeneration in adult zebrafish

Liping Ma,[1] Young-Mi Yu,[1] Yuji Guo,[1,3] Ronald P. Hart[1] and Melitta Schachner[1,2]
[1]W. M. Keck Center for Collaborative Neuroscience and Department of Cell Biology and Neuroscience, Rutgers, The State University of New Jersey, 604 Allison Road, Piscataway, NJ 08854, USA
[2]Center for Neuroscience, Shantou University Medical College, Shantou, China
[3]Department of Histology and Embryology, School of Medicine, Shandong University, China

Keywords: cysteine- and glycine-rich protein 1, microarray, nucleus of the medial longitudinal fascicle, spinal cord regeneration, zebrafish

Abstract

In contrast to mammals, adult zebrafish have the ability to regrow descending axons and gain locomotor recovery after spinal cord injury (SCI). In zebrafish, a decisive factor for successful spinal cord regeneration is the inherent ability of some neurons to regrow their axons via (re)expressing growth-associated genes during the regeneration period. The nucleus of the medial longitudinal fascicle (NMLF) is one of the nuclei capable of regenerative response after SCI. Using microarray analysis with laser capture microdissected NMLF, we show that cysteine- and glycine-rich protein (CRP)1a (encoded by the *csrp1a* gene in zebrafish), the function of which is largely unknown in the nervous system, was upregulated after SCI. *In situ* hybridization confirmed the upregulation of *csrp1a* expression in neurons during the axon growth phase after SCI, not only in the NMLF, but also in other nuclei capable of regeneration, such as the intermediate reticular formation and superior reticular formation. The upregulation of *csrp1a* expression in regenerating nuclei started at 3 days after SCI and continued to 21 days post-injury, the longest time point studied. *In vivo* knockdown of CRP1a expression using two different antisense morpholino oligonucleotides impaired axon regeneration and locomotor recovery when compared with a control morpholino, demonstrating that CRP1a upregulation is an important part of the innate regeneration capability in injured neurons of adult zebrafish. This study is the first to demonstrate the requirement of CRP1a for zebrafish spinal cord regeneration.

Introduction

In adult mammals, the failure of injured axons to regenerate after spinal cord injury (SCI) often results in permanent disabilities. Inhibitory molecules in the spinal cord are known to be major contributors to regeneration failure (David & Aguayo, 1981; Schwab & Bartholdi, 1996; Silver & Miller, 2004). However, removing inhibitory activities only induces limited axon regeneration that is insufficient for successful functional recovery (Zheng *et al.*, 2003; Case & Tessier-Lavigne, 2005; Yiu & He, 2006; Cafferty *et al.*, 2008), pointing to the importance of understanding the mechanisms for the intrinsic regenerative competence of neurons. Unlike mammals, adult zebrafish have the innate ability to regenerate descending axons after SCI, leading to locomotor recovery. In zebrafish, a crucial contributor to successful axon regeneration is the inherent ability of neurons to (re)express growth-associated genes and regrow their axons (Becker *et al.*, 1997, 2004; Bernhardt, 1999; Becker & Becker, 2008). *In vivo* depletion of these growth-associated genes dramatically impairs axon regeneration and locomotor recovery (Becker *et al.*, 2004; Yu *et al.*, 2011a,b). The ability to upregulate growth-associated genes during the regeneration period makes the adult zebrafish a valuable model for identifying molecules involved in successful spinal cord regeneration.

The nucleus of the medial longitudinal fascicle (NMLF), an anatomically well-defined nucleus, is one of several nuclei exhibiting a robust regenerative response after SCI as demonstrated by the upregulation of growth-associated genes and axonal regrowth (Becker *et al.*, 1997, 1998, 2004; Yu *et al.*, 2011a,b). To investigate the molecular mechanisms underlying this successful regeneration response, we performed microarray analysis with laser capture microdissected NMLF. The list of upregulated genes in the growth phase included known growth-associated genes, such as growth-associated protein 43 (GAP-43), as well as novel genes, the roles of which in axon regeneration are uncharacterized, such as cysteine- and glycine-rich protein (CRP)1.

Cysteine- and glycine-rich protein 1 is a member of the Lin11, Isl-1 and Mec-3-domain protein CRP family including CRP1 (CRP1a is encoded by the *csrp1a* gene in zebrafish), CRP2, and CRP3/muscle Lin11, Isl-1 and Mec-3-domain protein (Louis *et al.*, 1997). All CRP family members are highly expressed in muscle (Jain *et al.*, 1998) and CRP1 is regarded as a marker for smooth muscle cells (Henderson

Correspondence: Melitta Schachner, [2]Center for Neuroscience, Shantou University Medical College, as above. E-mail: schachner@biology.rutgers.edu

Received 30 May 2011, revised 7 November 2011, accepted 8 November 2011

et al., 1999). CRP1 is involved in many different cellular functions, acting as a transcriptional cofactor (Chang *et al.*, 2003), suppressing cell proliferation, protecting cells from stress-induced death (Latonen *et al.*, 2008), regulating cell movement during zebrafish development (Miyasaka *et al.*, 2007), and promoting neointima formation (Lilly *et al.*, 2010). CRP1 localizes to the nucleus and actin cytoskeleton (Tran *et al.*, 2005; Jang & Greenwood, 2009), and interacts with α-actinin (Pomies *et al.*, 1997) and zyxin (Sadler *et al.*, 1992; Schmeichel & Beckerle, 1998). CRP1 is the only CRP family member that has detectable expression in the mammalian central nervous system (Jain *et al.*, 1998). However, little is known about the functions of CRP1 in the central nervous system. In the present study, we report that *csrp1a* is upregulated after SCI and its expression *in vivo* is essential for successful axonal regeneration and locomotor recovery. Our results identify CRP1a as a key component of functional spinal cord regeneration in adult zebrafish.

Materials and methods

Spinal cord injury in adult zebrafish

Male adult zebrafish (*Danio rerio*, age > 6 months) were purchased from Aquatica Tropicals Inc. (Plant City, FL, USA). The fish were kept on a 14-h light and 10-h dark cycle at 28 °C.

The SCI was performed as described previously (Becker *et al.*, 1997, 2004; Guo *et al.*, 2011; Yu *et al.*, 2011a,b). Briefly, fish were immersed in 0.033% aminobenzoic acid ethylmethylester (MS222; Sigma, St Louis, MO, USA) for 5 min. After a longitudinal incision was made to expose the vertebral column, a complete transection of the spinal cord was performed between two vertebrae, about 1 mm (for microarray analysis and *in situ* hybridization) or 3.5 mm [for morpholino (MO) application] caudal to the brainstem–spinal cord junction, corresponding to the second and eighth vertebra, respectively. The number of animals used for each experiment can be found in the figure legends. The sham-lesioned control (CON) had identical surgical procedures except that the spinal cord was not cut. The wound was sealed with Histoacryl (B. Braun, Melsungen, Germany).

All animal experiments were carried out according to a protocol approved by the Rutgers University Institutional Animal Use and Care Committee, which conformed to NIH guidelines. Fish were killed with overdose anesthesia.

Laser capture microdissection, RNA isolation and amplification

A photoablation and laser microdissection system (Carl Zeiss, Thornwood, NY, USA) was used as previously described (Liss *et al.*, 2005). At 4 h, 12 h or 11 days after SCI, the brain was removed, embedded in Tissue-Tek optimal cutting temperature compound, and snap frozen in isopentane (cooled on dry ice). Utilizing the atlas of zebrafish brain (Wullimann *et al.*, 1996), coronal cryosections (20 μm) of zebrafish brainstem containing NMLF (approximately 30 sections) were cut and mounted on RNase-free, ultraviolet-light-treated, and poly-L-lysine-coated membrane slides (1 mm polyethylene/naphthalate membrane, photoablation and laser microdissection). Sections were fixed with ethanol (three washes with 70, 95 and 100% ethanol, respectively) and stained with 1% cresyl violet in 100% ethanol, and dried. The NMLF area was cut and captured directly into an adhesive cap (photoablation and laser microdissection). The buffer RLT (RNeasy Micro kit, Qiagen, Hilden, Germany) supplemented with β-mercaptoethanol (10 μL/mL) was added into the tube, which was then incubated upside-down for 30 min at 25 °C. Each condition (control or SCI) consisted of three microarrays. The RNA sample for each microarray was prepared from NMLF tissues pooled from three animals.

Total RNA was isolated using the RNeasy Micro kit (Qiagen) according to the manufacturer's directions with the addition of linear acrylamide (Ambion, Austin, TX, USA) as RNA carrier to the lysate. The RNA was amplified using the RampUP RNA amplification kit (Genisphere, Hatfield, PA, USA) following the manufacturer's protocol.

Microarray analysis and quantitative real-time polymerase chain reaction

Affymetrix GeneChip® Zebrafish Genome Arrays (Affymetrix, Santa Clara, CA, USA) containing 15 617 probes for ~14 900 transcripts were used for gene expression analysis, according to the manufacturer's instructions. Complementary DNA was reverse transcribed from the amplified RNA and hybridized to microarrays. Following hybridization, the arrays were washed and scanned following standard Affymetrix protocols. Data were extracted from CEL files using the robust multi-array average method (Irizarry *et al.*, 2003) as implemented in GeneSpring GX (Agilent, Santa Clara, CA, USA). The exploratory list (Table 1 and Supporting Information Table S1) was generated in GeneSpring by selecting genes with a *t*-test *P*-value of 0.05 or less and a fold change from control of 1.5 or more, both at 11 days after injury. The table (Table 1 and Supporting Information Table S1) lists average fold-change expression at each time point (calculated by taking the antilog of the log normalization values for each replicate array in GeneSpring) and the SEM. Data files have been deposited in the NIH Gene Expression Omnibus repository with the study accession number GSE28470. The link for the Gene Expression Omnibus dataset is https://www.ncbi.nlm.nih.gov/projects/geo/query/acc.cgi?acc=GSE28470.

Quantitative real-time polymerase chain reaction (qPCR) was performed with Power SYBR Green PCR Master Mix (Applied Biosystems, Foster City, CA, USA) as previously described (Goff *et al.*, 2004). The comparative cycle threshold C_t method ($\Delta\Delta C_t$ method) was used for data analysis. Results were expressed relative to control, sham-injured fish. The same cDNA used for the microarrays was used to test the expression of *GAP-43* and *csrp1a* in the NMLF after SCI. To study the expression of *csrp1a* in spinal cord caudal to the lesion site, total RNA was prepared from 4 mm pieces of whole spinal cord directly caudal to the lesion site. The primers used are as follows: zebrafish *csrp1a* (forward: 5′-TGCTTCCTGTGCATGGTTTG-3′; reverse: 5′-GGCCACCGTGGTACTGTCA-3′), zebrafish *GAP-43* (forward: 5′-TCAGGAGATCAAGCAGGATGG-3′; reverse: 5′-GCCTTGTGAGCGTTTTCCTC-3′) and zebrafish ribosomal protein *P0* (forward: 5′-TCGGCTACCCAACTCTTGCT-3′; reverse: 5′-TGTTTCGACAGTGACAGCCAG-3′).

In situ *hybridization*

Digoxigenin-labeled RNA sense and antisense probes for zebrafish *csrp1a* (NM_205567, 125–554 bp of coding sequence) were generated using the Megascript™ system (Ambion) according to the manufacturer's protocol and *in situ* hybridization was performed with some modifications as previously described (Becker *et al.*, 1998; Lieberoth *et al.*, 2003). No significant similarity was found with other zebrafish genes, demonstrating its specificity for *csrp1a*. Briefly, 20-μm-thick coronal sections containing the NMLF, intermediate reticular formation (IMRF) and superior reticular formation (SRF) were incubated with 0.1 N HCl for 10 min, followed by three washes

TABLE 1. List of selected genes upregulated in their expression in the NMLF at 11 days after SCI

			4 h		12 h		11 days	
Probe set ID	Gene symbol	Description	Control	Injured	Control	Injured	Control	Injured
Dr.967.1.S1_at	Mmp9	Matrix metalloproteinase 9	1.000 ± 0.084	1.493 ± 0.566	1.000 ± 0.162	1.186 ± 0.214	1.000 ± 0.157	10.438 ± 2.922
Dr.268.1.S1_at	epd	Ependymin	1.000 ± 0.670	0.762 ± 0.350	1.000 ± 0.168	2.200 ± 0.640	1.000 ± 0.324	8.402 ± 0.919
Dr.20019.1.S1_at	THY1	Thy-1 cell surface antigen	1.000 ± 0.106	1.141 ± 0.065	1.000 ± 0.198	0.980 ± 0.126	1.000 ± 0.243	6.358 ± 2.135
Dr.8236.1.S1_at	wnt4b	Wingless-type mouse mammary tumor virus (MMTV) integration site family, member 4b	1.000 ± 0.258	0.951 ± 0.363	1.000 ± 0.121	1.903 ± 0.832	1.000 ± 0.316	5.311 ± 0.787
Dr.9617.1.A1_at	socs3b	Suppressor of cytokine signaling 3b	1.000 ± 0.229	1.310 ± 0.072	1.000 ± 0.300	1.385 ± 0.419	1.000 ± 0.162	4.594 ± 0.512
Dr.14282.1.S1_at	atf3	Activating transcription factor 3	1.000 ± 0.148	1.763 ± 0.335	1.000 ± 0.167	1.682 ± 0.134	1.000 ± 0.332	3.908 ± 1.115
Dr.4416.1.A1_at	Tubb5	Tubulin, beta 5	1.000 ± 0.183	0.756 ± 0.139	1.000 ± 0.033	0.723 ± 0.122	1.000 ± 0.177	3.162 ± 0.306
Dr.10326.1.S1_at	junb	jun B proto-oncogene	1.000 ± 0.130	1.542 ± 0.252	1.000 ± 0.136	1.053 ± 0.074	1.000 ± 0.181	2.839 ± 0.460
Dr.8134.1.S1_at	PSME2	Proteasome activator subunit 2	1.000 ± 0.134	1.404 ± 0.092	1.000 ± 0.043	1.121 ± 0.104	1.000 ± 0.084	2.753 ± 0.321
Dr.2644.1.A1_at	dhrs3a	Dehydrogenase/reductase (short-chain dehydrogenase/reductase (SDR) family) member 3a	1.000 ± 0.137	1.642 ± 0.422	1.000 ± 0.154	1.602 ± 0.335	1.000 ± 0.228	2.728 ± 0.517
Dr.92.1.A1_at	gap43	Growth-associated protein 43	1.000 ± 0.188	0.907 ± 0.126	1.000 ± 0.02	0.884 ± 0.015	1.000 ± 0.111	2.304 ± 0.156
Dr.15857.1.A1_at	csrp1a	Cysteine- and glycine-rich protein 1	1.000 ± 0.137	1.200 ± 0.264	1.000 ± 0.026	1.008 ± 0.035	1.000 ± 0.148	1.714 ± 0.158
Dr.10428.1.S1_at	IRF7	Interferon regulatory factor 7	1.000 ± 0.051	1.375 ± 0.095	1.000 ± 0.038	1.157 ± 0.121	1.000 ± 0.116	1.689 ± 0.149
Dr.16078.1.S1_at	DCN	Decorin	1.000 ± 0.047	0.986 ± 0.119	1.000 ± 0.183	0.893 ± 0.130	1.000 ± 0.059	1.634 ± 0.108
Dr.12590.1.S1_at	jag1a	Jagged 1a	1.000 ± 0.138	0.883 ± 0.032	1.000 ± 0.015	0.972 ± 0.061	1.000 ± 0.061	1.536 ± 0.127
Dr.8145.1.S1_at	igf2a	Insulin-like growth factor 2a	1.000 ± 0.074	0.993 ± 0.040	1.000 ± 0.079	1.232 ± 0.033	1.000 ± 0.035	1.508 ± 0.095

in phosphate-buffered saline (PBS), pH 7.4, and then digested for 10 min with 10 μg/mL proteinase-K (Roche, Indianapolis, IN, USA) at room temperature, followed by two washes with glycine (2 mg/mL) in PBS, pH 7.4. Next, the sections were acetylated, dehydrated, air-dried, pre-hybridized, and subsequently hybridized with digoxigenin-labeled probe at 55 °C overnight. The hybridized probes were detected using alkaline phosphatase-coupled anti-digoxigenin antibody (Roche) and color developed with nitro-blue tetrazolium and 5-bromo-4-chloro-3-indolyl phosphate (Roche). The same development time was used for sections from control and SCI animals. *In situ* hybridization with the sense control probe was performed in parallel with the antisense probe on sections from injured animals, and no significant signal for the sense probe was observed. Neurons in the NMLF can be easily identified by their anatomical location according to the atlas of zebrafish brain (Wullimann *et al.*, 1996) and their large size (13–23 μm diameter) (Becker *et al.*, 1997), and are thus distinguishable from the small size of glial cells (Becker *et al.*, 1998). For profile counting, positively stained neurons in the NMLF, IMRF, or SRF from each animal were counted with the experimenter blinded to the treatment of each fish.

Double staining for in situ hybridization and immunohistochemistry

The labeling of cells coexpressing *csrp1a* (*in situ* hybridization) and the neuronal marker neuronal nuclei (NeuN) (immunohistochemistry) was performed after signal development by *in situ* hybridization. Slides were rinsed in PBS three times (5 min per wash) and antigen retrieval for immunohistochemistry was performed by incubation of the slides with 10 mM citrate buffer (pH 6.0) at 95 °C for 15 min as described previously (Ma *et al.*, 2006). The slides were then allowed to cool to room temperature. After three washes with PBS, the slides were blocked with 1% bovine serum albumin and 3% goat serum in PBS, and incubated with mouse anti-NeuN antibody (1 : 150, A-60, Millipore, Billerica, MA, USA) at 4 °C overnight. The slides were then washed three times in PBS and incubated with secondary antibody Alexa Fluor 555 (1 : 600, Invitrogen, Carlsbad, CA, USA).

Application of morpholinos and biocytin

Two different antisense MO oligonucleotides for zebrafish *csrp1a* (NM_205567) (*csrp1a* MO1: 5′-GTTTCCACCCCCAAGAGGCATC CTG-3′; *csrp1a* MO2: 5′-CTGCTAGGTGTGTGGATATGAAGAG-3′) were designed and synthesized by Gene Tools, LLC (Philomath, OR, USA). Both *csrp1a* MOs are directed to the start codon region to block translation. No significant similarity was found with other zebrafish genes, demonstrating their specificity for *csrp1a*. *Csrp1a* MO1 was tagged with carboxyfluorescein at the 3′ end. The specificity of *csrp1a* MO2 has been previously demonstrated and its effects on zebrafish embryos can be rescued by coinjection of *csrp1a* mRNA (Miyasaka *et al.*, 2007). *Csrp1a* MO2 could not be coupled with carboxyfluorescein due to its high G content, but was included to compare with previous studies. The sequence for the standard control MO, which was also tagged with carboxyfluorescein at the 3′ end, was 5′-CCTCTTACCTCAGTTACAATTTATA-3′. The MOs were dissolved in Danieau solution [58 mM NaCl, 0.7 mM KCl, 0.4 mM $MgSO_4$, 0.6 mM $Ca(NO_3)_2$, 5 mM HEPES, pH 7.6] and applied as previously described (Becker *et al.*, 2004; Guo *et al.*, 2011; Yu *et al.*, 2011a,b).

Fish were treated with 600 ng MO (approximately 0.27 μL, absorbed into Gelfoam, Upjohn, Kalamazoo, MI, USA) at the lesion site immediately after transection. The MO is taken up by lesioned

axons and retrogradely transported to the cells of origin in the brain, where protein synthesis for the target gene is blocked. The MO-treated fish were allowed to survive for 6 weeks. The dosing of the MOs (600 ng/fish) was chosen based our previous publication showing that 400 ng L1.1 MO is effective for knocking down protein expression and locomotor recovery in the identical zebrafish injury model (Becker *et al.*, 2004). Also, the effectiveness of this dosing has been confirmed by several publications from our group (Guo *et al.*, 2011; Yu *et al.*, 2011a,b).

At 6 weeks after the MO application, the neuronal tracer biocytin (Sigma)-saturated solution (approximately 0.27 μL, absorbed in Gelfoam) was applied to a secondary lesion site, which was 7 mm caudal to the brainstem–spinal cord junction, i.e. 3.5 mm caudal to the first spinal lesion site for MO application. Twenty-four hours later, the brains were dissected, embedded in optimal cutting temperature compound, and transversely frozen-sectioned. The biocytin was detected with the Vectastain ABC-DAB kit (Vector Laboratories, Burlingame, CA, USA) as previously described (Becker *et al.*, 1997; Yu *et al.*, 2011a). For profile counting, all positively stained neurons in the NMLF, IMRF, and SRF of each animal were counted with the experimenter blinded to the treatment of each fish.

Locomotor analysis

At 6 weeks after SCI and MO application (before the application of biocytin), the total distance moved by the MO-treated fish was measured to examine locomotor recovery. Tracking of freely moving fish was performed as previously described (Becker *et al.*, 2004; Guo *et al.*, 2011; Yu *et al.*, 2011a,b). Each fish was placed in a glass tank (50 × 30 cm) and allowed to move freely for 5 min while a video recording was captured using a camera mounted above the tank. Swim paths were tracked and calculated with the ANY-maze video tracking system (Stoelting Co., Wood Dale, IL, USA).

Western blot analysis

At 11 days after SCI and MO application as described above, a 2 mm section of spinal cord tissue, centered on the transection site, was dissected and lysed in radioimmunoprecipitation assay buffer (Sigma) supplemented with protease inhibitors (Roche). After homogenization, the lysate was pelleted and the protein concentration was determined with the bicinchoninic acid protein assay kit (Promega, Madison, WI, USA). Proteins were resolved on a 4–12% NuPAGE Bis-Tris gel (Invitrogen) and transferred to a polyvinylidene difluoride membrane. The blot was probed by a polyclonal CRP1 antibody produced in rabbit against the C-terminal of rat CRP1 (PKGFGFGQGA-GALVHSE) at 1.12 μg/mL. The antibody was a kind gift from Dr Greenwood (Oregon University, USA). α-Tubulin (1 : 1000, T9026, Sigma) served as a loading control on the same membrane after stripping. Horseradish peroxidase-conjugated goat anti-rabbit (Invitrogen, 1 : 5000) or horseradish peroxidase-conjugated goat anti-mouse (Millipore, 1 : 5000) were used as secondary antibodies. The enhanced chemiluminescence detection system (Pierce, Rockford, IL, USA) was used for signal detection. Quantitative analysis was performed using Kodak molecular imaging software version 4.0 (Carestream Molecular Imaging, New Haven, CT, USA).

Statistical analysis

Images were captured using a digital charge-coupled device camera attached to a microscope driven by AxioVision software (Zeiss). A two-tailed Student's *t*-test was used for results of microarray and qPCR of *GAP-43* and *csrp1a* in both NMLF and spinal cord, results of *csrp1a*-positive neuronal profiles in different regenerative nuclei at 11 days after SCI, and results of fluorescein-positive cell profiles of control MO and *csrp1a* MO1 at 6 weeks after MO application. One-way ANOVA followed by a Tukey's *post hoc* test when appropriate was used for results of densitometric analysis of CRP1a expression after MO application, results of locomotor recovery of fish after MO application, and results of neuronal profiles retrogradely labeled after MO application in different regenerative nuclei. Two-way ANOVA followed by a Tukey's *post hoc* test when appropriate was used for results of *csrp1a*-positive neuronal profiles in different regenerative nuclei at different time points. The level of significance was set at $P < 0.05$ for all analyses. Data are shown as mean values ± SEM. Statistical analyses were performed using R 2.12.2 (a free statistical software from http://www.r-project.org).

Results

Gene expression profiling of regenerating neurons in the nucleus of the medial longitudinal fascicle

In adult zebrafish, there are 20 distinct brain nuclei projecting to the spinal cord. Neurons in most brain nuclei grow axons beyond the transection site at 3.5 mm caudal to the brainstem–spinal cord transition zone (Becker *et al.*, 1997). It has been reported that different nuclei with the capacity to regenerate their axons have similar expression patterns for growth-associated genes, suggesting a shared molecular mechanism (Becker *et al.*, 1998). The NMLF neurons mount a robust regeneration response after SCI (Becker *et al.*, 1997, 1998, 2004; Yu *et al.*, 2011a,b). In addition, the NMLF is anatomically well defined, making it an excellent candidate to perform a screening assay such as microarray analysis. Spinal cord transection was performed at 1 mm caudal to the brainstem–spinal cord junction (Fig. 1). As the distance between the spinal cord and brainstem–spinal cord junction increases, the number of neurons in the brain projecting to the spinal cord decreases (Becker *et al.*, 1997). Thus, transection at the relatively rostral 1 mm level affects most neurons of the NMLF. Brain samples were collected at different time points to distinguish early (4 and 12 h) regulation in response to axotomy from regulation associated with the growth phase of descending axons (11 days). This time is when neurons increase the expression of growth-associated genes and exhibit active axon growth after SCI (Becker *et al.*, 1998, 2004). To concentrate the effect of injury response in relatively few cells within the region, laser capture microdissection was used to harvest NMLF from brain sections of sham-lesioned control or spinal cord-lesioned animals (Fig. 1). Because of the limited number of neurons in the NMLF and the small quantity of RNA recovered from captured NMLF, RNA amplification was performed and the resulting cDNA was used for microarray analysis (Fig. 1). Each condition (control or SCI) consisted of three microarrays, with the total RNA sample for each microarray prepared from laser-dissected NMLF tissues pooled from three animals.

The Zebrafish GeneChip microarray from Affymetrix was used for microarray analysis. As changes in gene expression at 11 days after SCI associate with the growth phase of descending axons, we initially tested for mRNA regulation due to axotomy injury at 11 days. When using a two-way ANOVA, no genes were found to be significantly affected by injury, probably due to the small fold changes and the limited number of arrays. However, to extract an exploratory list of potentially regulated genes, we selected 143 genes based solely on Student's *t*-test at $P \leq 0.05$ and a minimum 1.5-fold change

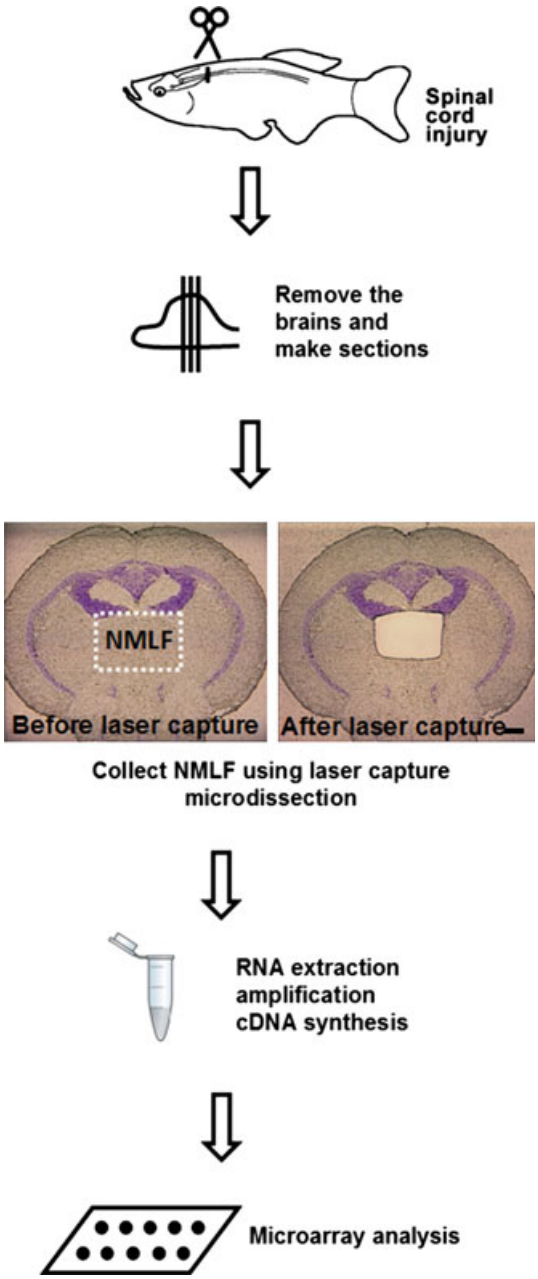

FIG. 1. Diagram of the work flow for microarray analysis. SCI was performed with a complete transection at 1 mm caudal to the brainstem–spinal cord junction. Brains were removed at different time points after SCI and sections were collected. After staining with cresyl violet, laser capture microdissection was used to isolate the NMLF. Total RNA was extracted from the pooled NMLF tissue and was amplified. cDNA from amplified RNA was used for microarray analysis. Scale bar, 1 mm.

(Supporting Information Table S1). The gene symbols and descriptions were obtained with DAVID (http://david.abcc.ncifcrf.gov/) (Huang da *et al.*, 2009a,b). The fold changes for gene expression in our microarray data were not as high as in, for instance, another study that used zebrafish retinal ganglion cells for microarray analysis (Veldman *et al.*, 2007), the reason for this probably being the small number of NMLF neurons (about 60) in each brain, and the presence of non-neuronal cells in the laser-dissected NMLF nucleus and/or other neurons that are not capable of regenerating after SCI, like cells in the nucleus ruber (Becker *et al.*, 1997). Table 1 lists a subset of upregulated genes from the exploratory list, selected based on published results linking their function to SCI or based on association with mechanisms thought to be prominent in SCI. As shown in Table 1, few of the genes upregulated at 11 days post-injury had changes in expression level in the early phase after axotomy, consistent with a specific role for those genes during the axon regeneration phase. This list contains several genes the roles of which have been reported in axon regeneration (outgrowth), including matrix metalloproteinase 9 (Vaillant *et al.*, 2003), GAP-43 (Skene, 1989; Leu *et al.*, 2010), activating transcription factor 3 (Seijffers *et al.*, 2006) and decorin (Davies *et al.*, 2004; Minor *et al.*, 2008). We used antisense MOs to study the functional roles of several of these genes proposed to be important for spinal cord regeneration, including *csrp1a*. As only *csrp1a* MO reduced the recovery of locomotor function, we chose to focus on this molecule.

Expression of csrp1a mRNA is upregulated in the nucleus of the medial longitudinal fascicle after spinal cord injury

If CRP1a is a growth-associated protein it should be regulated in parallel with other genes known to participate in regenerative mechanisms. GAP-43 is a well-known marker of axonal growth (Skene, 1989) and its expression is upregulated in different regenerating models (Bormann *et al.*, 1998; Costigan *et al.*, 2002; Veldman *et al.*, 2007). Expression of *GAP-43* mRNA is also upregulated in neurons of the NMLF and other nuclei capable of regeneration after SCI in adult zebrafish (Becker *et al.*, 1998). Here, GAP-43 is used as a positive control for genes that are upregulated after SCI. The microarray data showed that the normalized fold induction for *GAP-43* mRNA at 11 days after SCI was 2.3 (2.304 ± 0.156, $n = 3$ experiments, two-tailed *t*-test, $P = 0.003$) compared with the sham-lesioned control (CON), whereas the fold induction for *csrp1a* mRNA was 1.71 (1.714 ± 0.158, $n = 3$ experiments, two-tailed *t*-test, $P = 0.03$) (Fig. 2A). The upregulation of *GAP-43* and *csrp1a* expression in the microarray data was verified by qPCR, which showed that the fold induction values for *GAP-43* and *csrp1a* expression were 3.45 (3.45 ± 0.7, $n = 3$ experiments, two-tailed *t*-test, $P = 0.03$) and 1.44 (1.44 ± 0.1, $n = 3$ experiments, two-tailed *t*-test, $P = 0.01$), respectively (Fig. 2B). The discrepancy in the fold inductions between microarray and qPCR could be due to the difference in the amplification methods and detection techniques used in those assays; however, the reproduction of the upregulation by qPCR agrees with the predicted change observed on microarrays. *Csrp1a* expression is increased in NMLF after spinal axotomy, at a time when regenerative growth is observed.

In addition to neurons regenerating axons after SCI in the brain, the spinal cord region caudal to the lesion site, into which the regenerating axons must regrow, also contributes to the regenerative capacity (Becker *et al.*, 1998, 2004; Guo *et al.*, 2011). For example, expression of adhesion molecule L1.1 is upregulated in the caudal spinal cord after SCI and probably promotes spinal cord regeneration by acting not only in regrowing axons, but also in the caudal part of the injured spinal cord affecting, for instance, neuronal survival, axonal growth of interneurons and/or synaptic plasticity (Becker *et al.*, 2004). The expression of *csrp1a* mRNA in the spinal cord region caudal to the lesion site was therefore examined using qPCR to determine if it also functions in the regenerative milieu. Unlike the response found in the NMLF, the expression of *csrp1a* caudal to the lesion site was slightly decreased at 11 days after SCI (0.79 ± 0.02, $n = 3$ experiments, two-

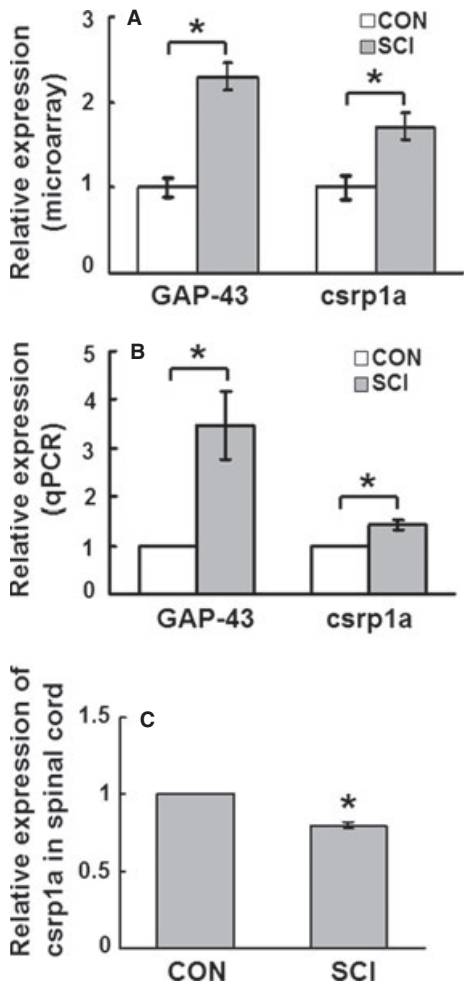

FIG. 2. *Csrp1a* mRNA expression is upregulated in the NMLF at 11 days after SCI. (A) Graph of normalized fold changes for *GAP-43* and *csrp1a* from microarray analysis. (B) qPCR shows that both *GAP-43* and *csrp1a* are upregulated in the NMLF at 11 days after SCI. (C) qPCR shows that *csrp1a* levels are slightly downregulated in the caudal part of the spinal cord at 11 days after SCI. $n = 3$ experiments. $^*P < 0.05$, two-tailed *t*-test; mean values ± SEM are shown.

tailed *t*-test, $P = 0.001$) (Fig. 2C). The downregulation of *csrp1a* expression after injury in the caudal part of the spinal cord could be related to the possibility that reduced levels in the regeneration-conducive tissue are associated with regrowth of axons. As *csrp1a* expression is upregulated in the NMLF, we conclude that this upregulation is mainly associated with the intrinsic regenerative response of neurons.

Csrp1a mRNA is upregulated in neurons of regenerative nuclei in the axon regeneration phase after spinal cord injury

The upregulation of *csrp1a* mRNA in individual NMLF neurons after SCI was determined by *in situ* hybridization. With the sense probe, no significant signal was observed when sections from injured animals were used in parallel with the antisense probe, i.e. under the same conditions. The NMLF neurons can be easily identified by their typical location and large size (13–23 μm in diameter) (Fig. 3A) (Wullimann *et al.*, 1996; Becker *et al.*, 1998, 2004), distinguishing them from glial cells, which are characterized by their small size (Becker *et al.*, 1998). Signal for *csrp1a* mRNA was observed in neurons in the NMLF (Figs 3 and 4). The expression of *csrp1a* in neurons was further confirmed by showing double labeling of *csrp1a* (*in situ* hybridization) and the neuronal marker NeuN (immunohistochemistry) in cells of the NMLF and the IMRF (Fig. 4). The number of *csrp1a*-positive neuronal profiles was strongly increased in the NMLF at 11 days after SCI (62.7 ± 5.7, $n = 6$ fish, two-tailed *t*-test, $P = 0.001$) (Fig. 3B) when compared with sham-lesioned control (12.7 ± 1, $n = 6$ fish). The expression of *csrp1a* mRNA was also studied in neurons from other nuclei capable of regeneration after SCI, such as the IMRF and SRF (Becker *et al.*, 1997). At 11 days post-injury, the numbers of *csrp1a*-positive cell profiles were increased in both the IMRF (119.3 ± 6.1, $n = 3$ fish, two-tailed *t*-test, $P = 0.001$, Fig. 3) and SRF (59.3 ± 4.5, $n = 3$ fish, two-tailed *t*-test, $P = 0.001$, Fig. 3) compared with sham-lesioned control (IMRF, 22.7 ± 4.3, $n = 3$ fish; SRF, 16 ± 1.5, $n = 3$ fish). In addition to the neurons of the regenerating nuclei studied, the expression of *csrp1a* was also examined in neurons of other nuclei with no or limited capacity for regeneration after SCI, such as Mauthner cells (Becker *et al.*, 1997). Interestingly, no significant upregulation of *csrp1a* expression was observed in Mauthner cells at 11 days after SCI (Fig. 4), similar to the observations on the adhesion molecule L1.1 (Becker *et al.*, 1998), suggesting that upregulation of *csrp1a* expression is specifically associated with regeneration. The upregulation of *csrp1a* mRNA in different regenerative nuclei after SCI is consistent with the prediction that similar molecular mechanisms are shared by different nuclei for regeneration (Becker *et al.*, 1998).

Next, a study was performed to investigate the regulation of *csrp1a* mRNA expression over time following SCI. As shown in Table 1, the expression of *csrp1a* did not change from sham injury at 4 and 12 h after axotomy, indicating that it is probably not involved in the early response after SCI. The expression of *csrp1a* at an additional two time points, 3 and 21 days after SCI, was studied using *in situ* hybridization. The number of *csrp1a*-positive neuronal profiles in the NMLF was slightly increased at 3 days after SCI. The expression of *csrp1a* was highly upregulated at 11 days (Figs 3 and 5). This upregulation continued to 21 days post-injury (Fig. 5A, SCI, 44 ± 3.7, $n = 3$ fish, two-way ANOVA followed by Tukey's *post hoc* test, $P = 0.002$; CON, 12.3 ± 1.8, $n = 3$ fish), the longest time point studied, albeit to a lesser extent than that of 11 days post-injury. Other nuclei capable of regeneration showed similar regulation pattern of *csrp1a* expression after SCI (IMRF, Fig. 5B; SRF, Fig. 5C). The upregulation of *csrp1a* mRNA in the growth phase of descending axons suggests that it may be a critical component of the neuron intrinsic regeneration response.

CRP1a is essential for spinal cord regeneration in zebrafish

Antisense MO oligonucleotides have been used effectively to investigate the role of specific genes in zebrafish spinal cord regeneration (Becker *et al.*, 2004; Guo *et al.*, 2011; Yu *et al.*, 2011a,b). Like conventional neuronal tracers, MO can be absorbed by the injured axons at the lesion site and retrogradely transported into neuronal somata where the protein translation of the target gene is blocked. In the zebrafish SCI model, this can be accomplished by placing MO-soaked Gelfoam into the spinal cord transection site. The inhibitory effect of MO can last for at least 6 weeks (the longest time point tested) (Becker *et al.*, 2004). Gelfoam alone or with the standard control MO did not show any effect on neuronal viability or spinal cord regeneration (Becker *et al.*, 2004).

The role of a gene in zebrafish spinal cord regeneration has been evaluated by two definitive parameters: locomotor recovery and

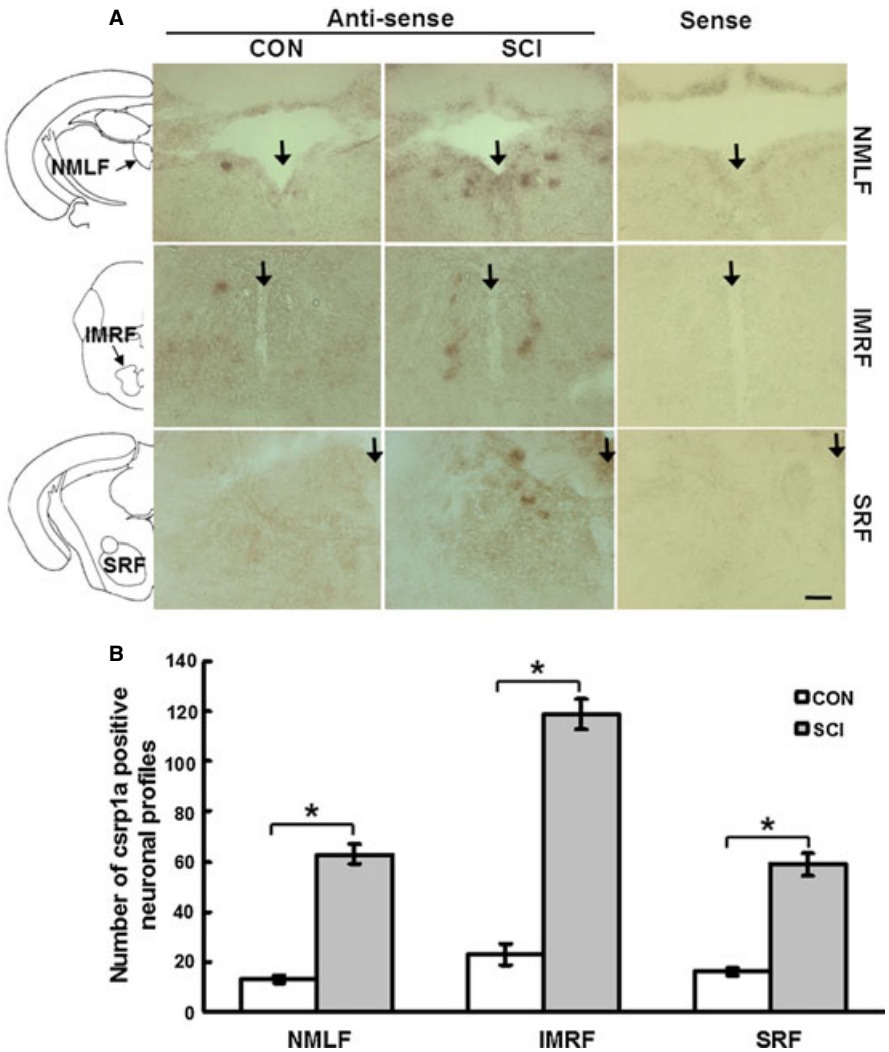

FIG. 3. *Csrp1a* mRNA expression is upregulated in the NMLF, IMRF and SRF at 11 days after SCI. (A) *In situ* hybridization was performed to study the expression of *csrp1a* in regenerative nuclei. Representative images depict *csrp1a*-positive neurons in the NMLF, IMRF and SRF at 11 days after SCI. Schematic drawings of the NMLF, IMRF and SRF are shown. Positive signal for *csrp1a* mRNA is observed in neurons, i.e. cells with a diameter of more than 13 μm. More positive neurons for *csrp1a* were observed in all three nuclei after SCI when compared with sham-lesioned control. With sense probe, no significant signal was observed. Arrows in the schematic drawings indicate the corresponding nucleus. Arrows in images indicate the brain midline. (B) Quantification shows that *csrp1a* is upregulated in the NMLF, IMRF and SRF at 11 days after SCI. NMLF, $n = 6$ fish; IMRF, $n = 3$ fish; SRF, $n = 3$ fish. $^*P < 0.05$, two-tailed *t*-test; mean values ± SEM are shown. Scale bar, 50 μm.

axonal regrowth (Becker *et al.*, 2004; Yu *et al.*, 2011a,b). The total distance moved by fish in 5 min is used to measure locomotor activity. The locomotor activity is reduced to approximately 5% of that in unlesioned fish at 1 week after SCI and generally recovers to 60% at 6 weeks. No additional improvement is observed after this point (Becker *et al.*, 2004). The identification of neurons that have regenerated their axons beyond the lesion site is performed by applying the retrograde tracer biocytin at 3.5 mm caudal to the transection site at 6 weeks after the lesion. The degree of locomotor recovery and the number of retrogradely labeled neurons reflect the extent of spinal cord regeneration and these two parameters are usually correlated (Becker *et al.*, 2004).

The role of CRP1a in spinal cord regeneration was investigated using two different MOs specific for *csrp1a*. The effectiveness of the two *csrp1a* MOs used was examined by western blot analysis. The CRP1 antibody used here detected only one band of the correct size for CRP1a, demonstrating its specificity (Fig. 6A). Signal for CRP1a was detected with samples from both brain and spinal cord, confirming the expression of *csrp1a* as shown by *in situ* hybridization. To test the effectiveness of *csrp1a* MOs, a 2 mm section of spinal cord tissue, centered on the transection site, was collected at 11 days after MO application and examined by western blot analysis. Both *csrp1a* MO1 and *csrp1a* MO2 exhibited effective knockdown of CRP1a expression compared with the control MO, with a knockdown of 30% ($n = 3$ experiments, one-way ANOVA followed by Tukey's *post hoc* test, $P = 0.01$) and 40% ($n = 3$ experiments, one-way ANOVA followed by Tukey's *post hoc* test, $P = 0.01$), respectively (Fig. 6B and C). Thus, both *csrp1a* MOs worked effectively in our system.

At 6 weeks after SCI, fish treated with *csrp1a* MO1 showed a decrease in the total distance moved (278 ± 104 cm/5 min, $n = 12$ fish, one-way ANOVA followed by Tukey's *post hoc* test, $P = 0.003$, Fig. 6D) compared with fish treated with control MO (1108 ± 365 cm/5 min, $n = 9$ fish). *Csrp1a* MO2 treatment exhibited a similar effect (261 ± 97 cm/5 min, $n = 5$ fish, one-way ANOVA

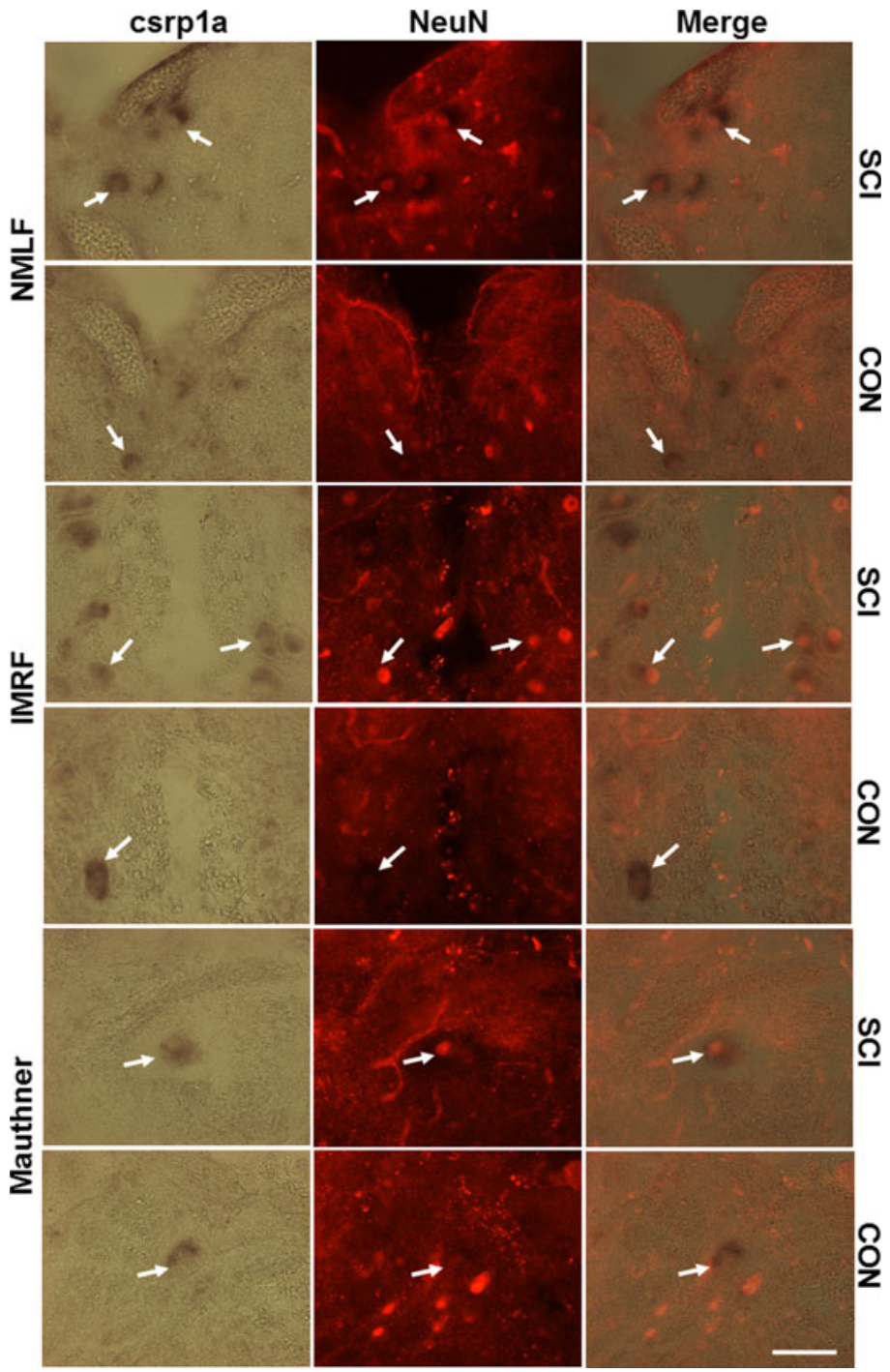

FIG. 4. *Csrp1a* mRNA expression is upregulated in NeuN-positive neurons in regenerative nuclei after SCI. Double staining of *csrp1a* mRNA (*in situ* hybridization) and NeuN (immunohistochemistry) was performed to determine the identity of *csrp1a*-positive cells. The signal for NeuN locates in the nucleus and *csrp1a* locates in the cytoplasm. Cells positive for *csrp1a* mRNA are also labeled by NeuN, demonstrating that *csrp1a* is expressed by neurons. More double-labeling cells are observed at 11 days after SCI in regenerative nuclei, such as the NMLF (upper two rows) and IMRF (middle two rows), when compared with control, whereas no significant upregulation of *csrp1a* expression is found after SCI in Mauthner cells (lower two rows), which are not capable of regenerating after SCI. $n = 3$ experiments. Scale bar, 50 μm.

followed by Tukey's *post hoc* test, $P = 0.008$, Fig. 6D). *Csrp1a* MO2 has been used to knockdown CRP1a expression and its specificity has been confirmed with a *csrp1a* mRNA rescue experiment (Miyasaka *et al.*, 2007). These data indicate that *csrp1a* MOs impaired locomotor recovery. After locomotor analysis, the same fish were used to retrogradely label neurons that had regrown their axons 3.5 mm beyond the lesion site. The number of neuronal profiles retrogradely labeled in the NMLF was reduced in animals treated with *csrp1a* MO1 (11 ± 2.3, $n = 12$ fish, one-way ANOVA followed by Tukey's *post hoc* test, $P = 0.001$) or *csrp1a* MO2 (13.2 ± 4.3, $n = 5$ fish, one-way ANOVA followed by Tukey's *post hoc* test, $P = 0.01$) compared with fish treated with control MO (27.7 ± 2.9, $n = 10$ fish) (Fig. 7A and

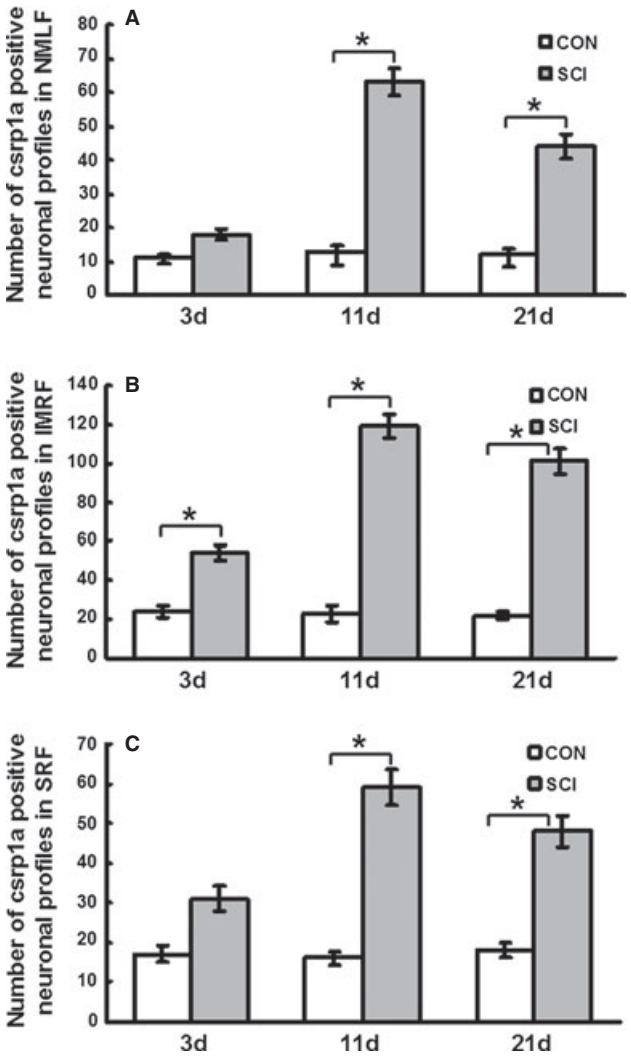

FIG. 5. *Csrp1a* mRNA expression is upregulated in the axon regeneration phase after SCI. *In situ* hybridization was performed to investigate the regulation pattern of *csrp1a* mRNA expression after SCI. Three different time points were included: 3, 11 and 21 days after SCI. Quantification shows that *csrp1a* mRNA is slightly upregulated at 3 days. The expression of *csrp1a* mRNA is highly induced at 11 days post-injury and this upregulation continues to 21 days, the longest time point tested. Similar regulation patterns of *csrp1a* expression are observed in the NMLF (A), IMRF (B) and SRF (C). $n = 3$ fish for each time point. $^*P < 0.05$, two-way ANOVA with Tukey's *post hoc* test; mean values ± SEM are shown.

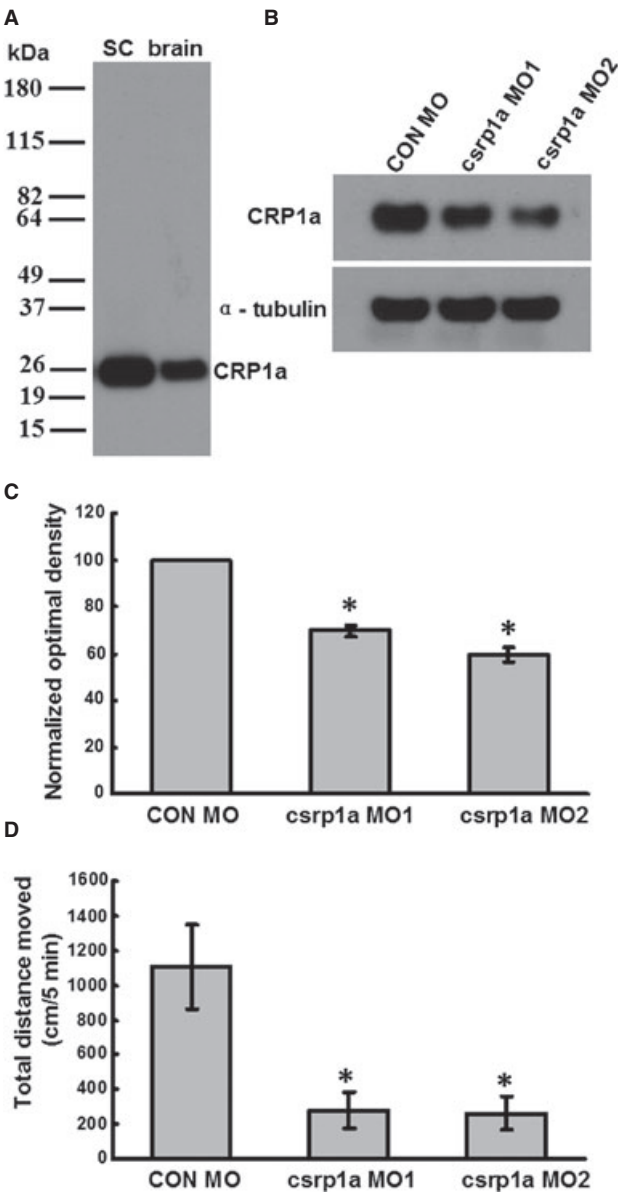

FIG. 6. Application of *csrp1a* MOs inhibits locomotor recovery after SCI. (A) The CRP1a antibody used for western blot analysis only detects one band of the correct size for CRP1a, demonstrating the specificity of the antibody. Signal for CRP1a was detected with both samples from zebrafish spinal cord (SC) and brain. (B and C) *Csrp1a* MO1 and *csrp1a* MO2 knockdown CRP1a expression. A 2 mm section of SC tissue, centered on the transection site, was collected at 11 days after SCI and MO application. α-tubulin serves as a loading control. *Csrp1a* MO1 and *csrp1a* MO2 exhibited 30 and 40% knockdown effect of CRP1a expression compared with control MO, respectively, as demonstrated by western blot analysis (B) and densitometric analysis (C). (D) Total distance moved by animals treated with CON MO, *csrp1a* MO1, or *csrp1a* MO2 was measured during 5 min trial periods by video recording at 6 weeks after MO application. *csrp1a* MO1 ($n = 12$ fish) or *csrp1a* MO2 ($n = 5$ fish) treatments reduce the total distance moved when compared with CON MO treatment ($n = 9$ fish). (A-C) $n = 3$ experiments. $^*P < 0.05$, one-way ANOVA with Tukey's *post hoc* test; mean values ± SEM are shown.

B). *Csrp1a* MOs treatments also reduced the number of neuronal profiles retrogradely labeled in the IMRF (Fig. 7A and B, *csrp1a* MO1, 15.3 ± 3.4, $n = 4$ fish, one-way ANOVA followed by Tukey's *post hoc* test, $P = 0.02$; *csrp1a* MO2, 13.8 ± 2.8, $n = 5$ fish, one-way ANOVA followed by Tukey's *post hoc* test, $P = 0.01$; CON MO, 36 ± 6.8, $n = 3$ fish) and SRF (Fig. 7A and B, *csrp1a* MO1, 6.8 ± 1.8, $n = 4$ fish, one-way ANOVA followed by Tukey's *post hoc* test, $P = 0.02$; *csrp1a* MO2, 9.4 ± 2.7, $n = 5$ fish, one-way ANOVA followed by Tukey's *post hoc* test, $P = 0.03$; CON MO, 25 ± 6.6, $n = 3$ fish). These data suggest that knockdown of CRP1a inhibits locomotor recovery and axonal regrowth after SCI.

We then asked whether the reduced number of neuronal profiles retrogradely labeled is due to reduced cell viability after MO application. In this study, both the standard MO and *csrp1a* MO1 were tagged with fluorescein, which does not affect cell viability and spinal cord regeneration (Becker *et al.*, 2004). No effect on cell viability by *csrp1a* MO2 has been reported (Miyasaka *et al.*, 2007). Because of the inappropriateness of *csrp1a* MO2 being coupled with the fluorescein tag due to its high G content, it is not included in this experiment. In agreement with previous findings (Becker *et al.*, 2004),

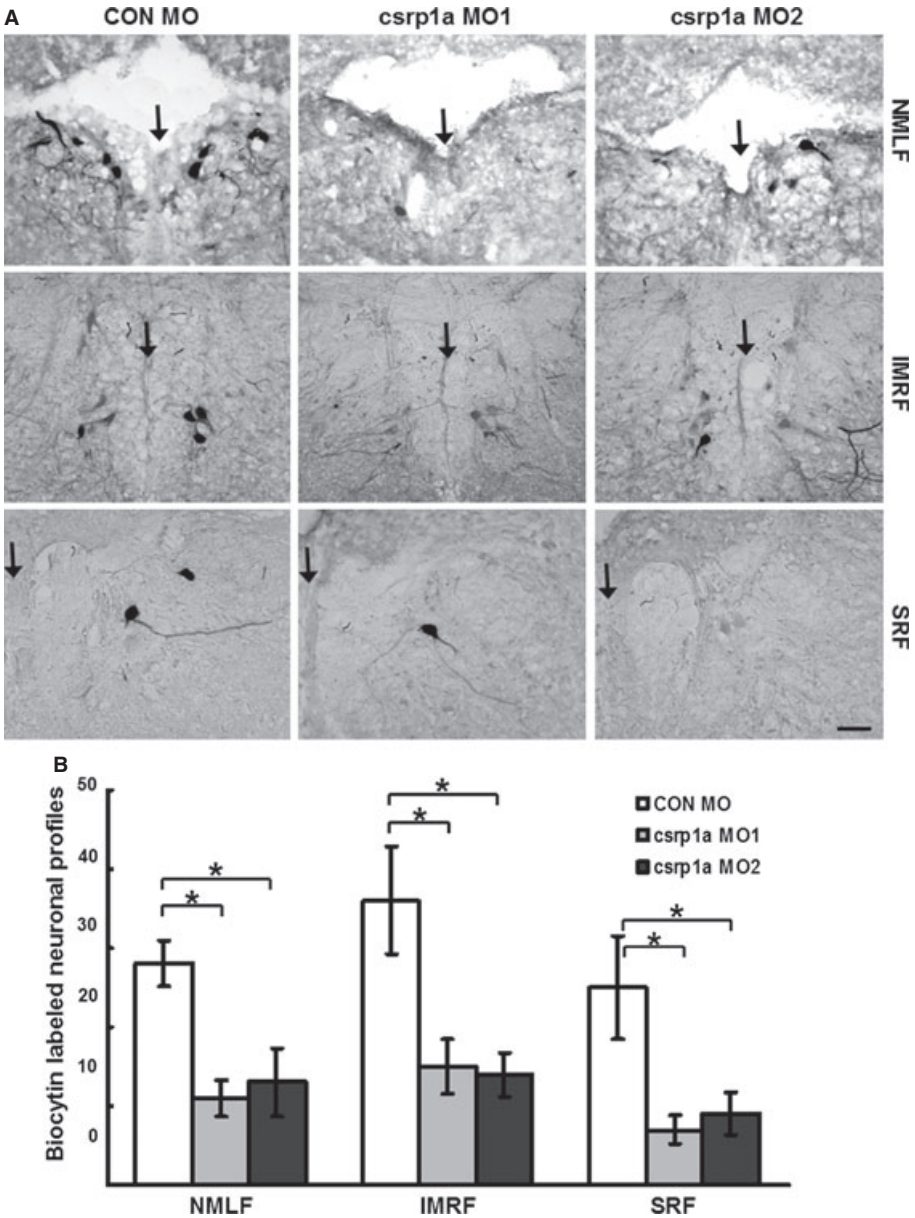

FIG. 7. *Csrp1a* MOs inhibit axon regeneration after SCI. (A) Representative images of retrogradely labeled neurons in the NMLF, IMRF and SRF. The number of retrogradely labeled neuronal profiles in the NMLF, IMRF and SRF (biocytin label) is measured at 6 weeks after SCI and MO application. Biocytin was applied at 3.5 mm caudal to the lesion site and was detected 24 h later. *Csrp1a* MO1 and *csrp1a* MO2 treatments reduce the number of biocytin-labeled neuronal profiles in all nuclei studied when compared with the CON MO. Arrows in images indicate the brain midline. (B) Quantification shows a reduction in numbers of biocytin-labeled neuronal profiles in fish that received *csrp1a* MO1 or *csrp1a* MO2 compared with fish that received CON MO. $*P < 0.05$, one-way ANOVA with Tukey's *post hoc* test; mean values ± SEM are shown. Scale bar, 50 μm.

the fluorescein tag signal on the MOs was still detectable in the NMLF neurons at 6 weeks after application. As standard control MO does not show an effect on cell viability (Becker *et al.*, 2004), we compared the number of fluorescein-positive cell profiles from *csrp1a* MO1-treated fish with that from control MO-treated fish. No difference was found in the numbers of fluorescein-positive cell profiles in the NMLF between control and experimental animals (control MO, 25 ± 3.8, $n = 3$ fish; *csrp1a* MO1, 24 ± 4.8, $n = 4$ fish, two-tailed *t*-test, $P = 0.85$) (Fig. 8), indicating that neurons survived the *csrp1a* MO1 and control MO applications equally well. Similar results were observed in the IMRF and SRF (data not shown). In all, the combined observations showed reduced locomotor recovery and reduced numbers of retrogradely labeled NMLF neurons in animals treated with *csrp1a* MO, indicating that CRP1a is required for successful spinal cord regeneration in zebrafish.

Discussion

Unlike mammals, adult zebrafish have the innate ability to (re)express growth-associated genes and regenerate descending axons after SCI leading to locomotor recovery (Becker *et al.*, 1997, 1998, 2004; Bernhardt, 1999). However, the molecular mechanisms for successful spinal cord regeneration have not been fully explored. In the current study, microarray analysis was used to obtain an exploratory list of

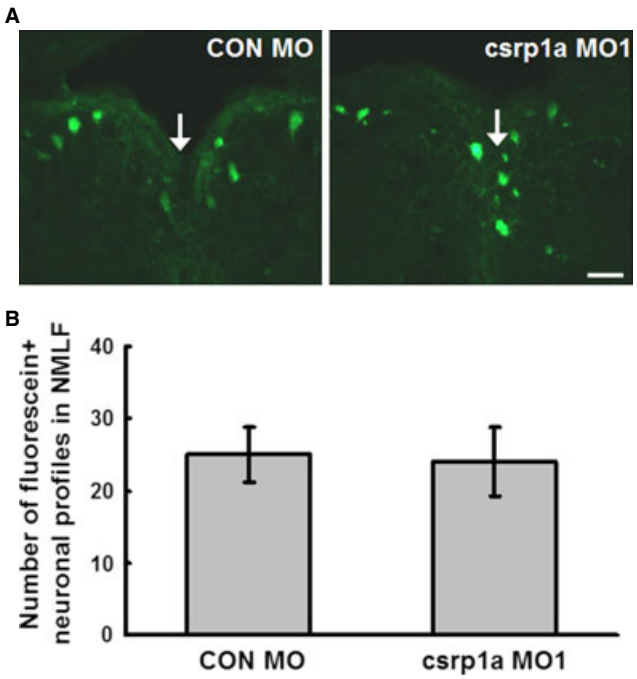

FIG. 8. *Csrp1a* MO1 does not affect cell viability. (A) Representative images of neurons with fluorescein signal in the NMLF at 6 weeks after MO application. The standard control MO and *csrp1a* MO1 were tagged with fluorescein and this signal is still detectable at 6 weeks after MO application. No difference was found between the numbers of fluorescein-positive neuronal profiles in animals treated with CON MO or *csrp1a* MO1. Arrows in images indicate the brain midline. (B) Quantification shows no difference in the numbers of fluorescein-positive neuronal profiles in the NMLF in animals treated with CON MO ($n = 3$ fish) or *csrp1a* MO1 ($n = 4$ fish). Mean values ± SEM are shown. Scale bar, 50 μm.

potential growth-associated genes from regenerating NMLF. Among the potentially upregulated genes during the axon regeneration phase, several have been reported to be induced during the regeneration period after nerve injury (Veldman *et al.*, 2007; McCurley & Callard, 2010; Saul *et al.*, 2010; Siebert *et al.*, 2010), such as matrix metalloproteinase 9, GAP-43, activating transcription factor 3, tubulin beta 5 and suppressor of cytokine signaling 3b, supporting the validity of this analysis. Furthermore, some of the identified genes appear to be specifically regulated in adult vertebrates competent for spinal cord regeneration. Decorin is a small, leucine-rich proteoglycan that has previously been shown to promote axon growth across adult rat SCIs (Davies *et al.*, 2004). Decorin also promotes robust axon growth on chondroitin sulfate proteoglycans and myelin (Minor *et al.*, 2008), two major inhibitory factors for axon regeneration within the adult mammalian central nervous system (Morgenstern *et al.*, 2002; Yiu & He, 2006). Our microarray shows that decorin is probably upregulated during the axonal regeneration period after SCI in adult zebrafish (11 days). However, to the best of our knowledge, the upregulation of decorin has not been reported in other microarray analysis after nerve injury in adult mammals (Veldman *et al.*, 2007; McCurley & Callard, 2010; Saul *et al.*, 2010; Siebert *et al.*, 2010; Gibbs *et al.*, 2011), indicating it as one of the specific genes involved in spinal cord regeneration. However, L1.1, a well-known adhesion molecule for axon regeneration, was not found on our list. Although our microarray analysis showed a 1.82-fold change for L1.1 at 11 days after SCI, the result was not significant when compared with the control group (with 0.42 for the *P* value), probably due to a combination of measurement variability, low signal, and the limited number of replicates. Variability could be due to the limited number of regenerative neurons in the tissue sample, the presence of other non-regenerative cells and the possible technical variation added by the two-step RNA amplification procedures involved in RNA preparation for microarray. Due to these limitations, our list may not include all of the upregulated mRNAs after SCI.

Quantitative PCR confirms predictions from the microarray, showing that both *GAP-43* and *csrp1a* are upregulated in the regenerating NMLF during the growth phase after SCI. Similarly, upregulation of CRP1 has also been reported in heart regeneration (Lien *et al.*, 2006), fin regeneration (Schebesta *et al.*, 2006) and optic nerve regeneration (McCurley & Callard, 2010), indicating CRP1 expression as a common molecular mechanism for regeneration. The upregulation of *csrp1a* in neurons in several regenerative nuclei after axotomy was confirmed by *in situ* hybridization. *In vivo* knockdown of CRP1a expression with specific MOs impaired both locomotor recovery and axon regeneration, demonstrating that CRP1a upregulation is an essential part of the natural regeneration mechanism in spinal cord-injured adult zebrafish. Successful spinal cord regeneration requires at least two critical factors: the ability of an injured neuron to regrow its axon and a supportive extracellular environment for axon regeneration (Bulsara *et al.*, 2002). In addition, rearrangements of the intraspinal connections of interneurons involving pre-synaptic and post-synaptic structures need to be considered (Guo *et al.*, 2011). Interestingly, *csrp1a* levels are only upregulated in the cell bodies of neurons regenerating axons, but not in the caudal part of the spinal cord, into which the severed axons regrow. This suggests that the upregulation of CRP1a is only associated with the neuron-intrinsic regeneration response and its upregulation is not required in the extrinsic response that generates a permissive environment for axon regeneration. Thus, we propose that the effect of *csrp1a* MOs on spinal cord regeneration is mainly due to the loss of CRP1a expression in those neurons that regrow their severed axons.

As a Lin11, Isl-1 and Mec-3-domain protein, CRP1 plays a role in many different functions, such as gene transcription, cell movements, and cell proliferation (Chang *et al.*, 2003; Miyasaka *et al.*, 2007; Latonen *et al.*, 2008). The amino acid sequence of CRP1 is very similar among vertebrates with more than 80% identity between human, mouse, rat, chicken, quail and zebrafish, suggesting its conserved function over evolution (McLaughlin *et al.*, 1994). It has been reported that CRP1 binds actin filaments directly and cross-links them to generate actin bundles (Tran *et al.*, 2005; Jang & Greenwood, 2009). Actin bundles are the major component of filopodia at the leading edge of growth cones. Filopodia formation is critical for neurite outgrowth, neuritogenesis, neurite branching and spine formation in neurons (Mattila & Lappalainen, 2008). Expression of CRP1 in filopodia of growth cones and colocalization with actin filaments was observed by indirect immunofluorescence in cultured rat hippocampal neurons (Ma *et al.*, 2011), which is consistent with its reported actin-bundling ability (Tran *et al.*, 2005; Jang & Greenwood, 2009). Therefore, we propose that the role of CRP1a in spinal cord regeneration is probably due to its actin-bundling activity in filopodia formation. As filopodia formation affects several different aspects of neurite modeling, such as axon outgrowth (Kwiatkowski *et al.*, 2007), neuritogenesis (Dent *et al.*, 2007) and neurite branching (Dailey & Smith, 1996), one or more of the aspects mentioned above may contribute to the requirement of CRP1a in spinal cord regeneration in zebrafish.

In addition to the interaction of CRP1 with the cytoskeleton, the involvement of CRP1 in other pathways has been reported. For example, it has been shown that CRP1 is involved in activation of the c-jun N-terminal kinase pathway and interacts with Diversin and

Dishevelled 2 (Miyasaka *et al.*, 2007). Moreover, it has been reported that CRP1 acts as a cofactor together with SRF to activate the transcription of target genes in smooth muscle (Chang *et al.*, 2003). Further investigations are needed to elucidate whether these mechanisms of CRP1 underlie successful spinal cord regeneration in zebrafish.

Supporting Information

Additional supporting information can be found in the online version of this article:

Table S1. List of potentially upregulated genes in the NMLF at 11 days after SCI.

Please note: As a service to our authors and readers, this journal provides supporting information supplied by the authors. Such materials are peer-reviewed and may be re organized for online delivery, but are not copy-edited or typeset by Wiley-Blackwell. Technical support issues arising from supporting information (other than missing files) should be addressed to the authors.

Acknowledgements

We are very grateful to K. M. Gibbs for his helpful comments on the manuscript and J. A. Greenwood for the kind gift of CRP1 antibody. We also thank Brian Siwek for his diligent care of the fish. This work was supported by a grant from the New Jersey Commission on Spinal Cord Research (05-3048-SCR-E-0 to M.S.). M.S. is New Jersey Professor of Spinal Cord Research and a consultant at the Center for Neuroscience of the Li Kashing Shantou University Medical College, China.

Abbreviations

CON, control; CRP, cysteine- and glycine-rich protein (CRP1a is encoded by the *csrp1a* gene in zebrafish); GAP-43, growth-associated protein 43; IMRF, intermediate reticular formation; MO, morpholino; NeuN, neuronal nuclei; NMLF, nucleus of the medial longitudinal fascicle; PBS, phosphate-buffered saline; qPCR, quantitative real-time polymerase chain reaction; SCI, spinal cord injury; SRF, superior reticular formation.

References

Becker, C.G. & Becker, T. (2008) Adult zebrafish as a model for successful central nervous system regeneration. *Restor. Neurol. Neurosci.*, **26**, 71–80.

Becker, T., Wullimann, M.F., Becker, C.G., Bernhardt, R.R. & Schachner, M. (1997) Axonal regrowth after spinal cord transection in adult zebrafish. *J. Comp. Neurol.*, **377**, 577–595.

Becker, T., Bernhardt, R.R., Reinhard, E., Wullimann, M.F., Tongiorgi, E. & Schachner, M. (1998) Readiness of zebrafish brain neurons to regenerate a spinal axon correlates with differential expression of specific cell recognition molecules. *J. Neurosci.*, **18**, 5789–5803.

Becker, C.G., Lieberoth, B.C., Morellini, F., Feldner, J., Becker, T. & Schachner, M. (2004) L1.1 is involved in spinal cord regeneration in adult zebrafish. *J. Neurosci.*, **24**, 7837–7842.

Bernhardt, R.R. (1999) Cellular and molecular bases of axonal regeneration in the fish central nervous system. *Exp. Neurol.*, **157**, 223–240.

Bormann, P., Zumsteg, V.M., Roth, L.W. & Reinhard, E. (1998) Target contact regulates GAP-43 and alpha-tubulin mRNA levels in regenerating retinal ganglion cells. *J. Neurosci. Res.*, **52**, 405–419.

Bulsara, K.R., Iskandar, B.J., Villavicencio, A.T. & Skene, J.H. (2002) A new millenium for spinal cord regeneration: growth-associated genes. *Spine (Phila Pa 1976)*, **2002**, 1946–1949.

Cafferty, W.B., McGee, A.W. & Strittmatter, S.M. (2008) Axonal growth therapeutics: regeneration or sprouting or plasticity? *Trends Neurosci.*, **31**, 215–220.

Case, L.C. & Tessier-Lavigne, M. (2005) Regeneration of the adult central nervous system. *Curr. Biol.*, **15**, R749–R753.

Chang, D.F., Belaguli, N.S., Iyer, D., Roberts, W.B., Wu, S.P., Dong, X.R., Marx, J.G., Moore, M.S., Beckerle, M.C., Majesky, M.W. & Schwartz, R.J. (2003) Cysteine-rich LIM-only proteins CRP1 and CRP2 are potent smooth muscle differentiation cofactors. *Dev. Cell*, **4**, 107–118.

Costigan, M., Befort, K., Karchewski, L., Griffin, R.S., D'Urso, D., Allchorne, A., Sitarski, J., Mannion, J.W., Pratt, R.E. & Woolf, C.J. (2002) Replicate high-density rat genome oligonucleotide microarrays reveal hundreds of regulated genes in the dorsal root ganglion after peripheral nerve injury. *BMC Neurosci.*, **3**, 16.

Dailey, M.E. & Smith, S.J. (1996) The dynamics of dendritic structure in developing hippocampal slices. *J. Neurosci.*, **16**, 2983–2994.

David, S. & Aguayo, A.J. (1981) Axonal elongation into peripheral nervous system ''bridges'' after central nervous system injury in adult rats. *Science*, **214**, 931–933.

Davies, J.E., Tang, X., Denning, J.W., Archibald, S.J. & Davies, S.J. (2004) Decorin suppresses neurocan, brevican, phosphacan and NG2 expression and promotes axon growth across adult rat spinal cord injuries. *Eur. J. Neurosci.*, **19**, 1226–1242.

Dent, E.W., Kwiatkowski, A.V., Mebane, L.M., Philippar, U., Barzik, M., Rubinson, D.A., Gupton, S., Van Veen, J.E., Furman, C., Zhang, J., Alberts, A.S., Mori, S. & Gertler, F.B. (2007) Filopodia are required for cortical neurite initiation. *Nat. Cell Biol.*, **9**, 1347–1359.

Gibbs, K.M., Chittur, S.V. & Szaro, B.G. (2011) Metamorphosis and the regenerative capacity of spinal cord axons in Xenopus laevis. *Eur. J. Neurosci.*, **33**, 9–25.

Goff, L.A., Bowers, J., Schwalm, J., Howerton, K., Getts, R.C. & Hart, R.P. (2004) Evaluation of sense-strand mRNA amplification by comparative quantitative PCR. *BMC Genomics*, **5**, 76–84.

Guo, Y., Ma, L., Cristofanilli, M., Hart, R.P., Hao, A. & Schachner, M. (2011) Transcription factor Sox11b is involved in spinal cord regeneration in adult zebrafish. *Neuroscience*, **172**, 329–341.

Henderson, J.R., Macalma, T., Brown, D., Richardson, J.A., Olson, E.N. & Beckerle, M.C. (1999) The LIM protein, CRP1, is a smooth muscle marker. *Dev. Dyn.*, **214**, 229–238.

Huang da, W., Sherman, B.T. & Lempicki, R.A. (2009a) Bioinformatics enrichment tools: paths toward the comprehensive functional analysis of large gene lists. *Nucleic Acids Res.*, **37**, 1–13.

Huang da, W., Sherman, B.T. & Lempicki, R.A. (2009b) Systematic and integrative analysis of large gene lists using DAVID bioinformatics resources. *Nat. Protoc.*, **4**, 44–57.

Irizarry, R.A., Hobbs, B., Collin, F., Beazer-Barclay, Y.D., Antonellis, K.J., Scherf, U. & Speed, T.P. (2003) Exploration, normalization, and summaries of high density oligonucleotide array probe level data. *Biostatistics*, **4**, 249–264.

Jain, M.K., Kashiki, S., Hsieh, C.M., Layne, M.D., Yet, S.F., Sibinga, N.E., Chin, M.T., Feinberg, M.W., Woo, I., Maas, R.L., Haber, E. & Lee, M.E. (1998) Embryonic expression suggests an important role for CRP2/SmLIM in the developing cardiovascular system. *Circ. Res.*, **83**, 980–985.

Jang, H.S. & Greenwood, J.A. (2009) Glycine-rich region regulates cysteine-rich protein 1 binding to actin cytoskeleton. *Biochem. Biophys. Res. Commun.*, **380**, 484–488.

Kwiatkowski, A.V., Rubinson, D.A., Dent, E.W., Edward van Veen, J., Leslie, J.D., Zhang, J., Mebane, L.M., Philippar, U., Pinheiro, E.M., Burds, A.A., Bronson, R.T., Mori, S., Fassler, R. & Gertler, F.B. (2007) Ena/VASP is required for neuritogenesis in the developing cortex. *Neuron*, **56**, 441–455.

Latonen, L., Jarvinen, P.M. & Laiho, M. (2008) Cytoskeleton-interacting LIM-domain protein CRP1 suppresses cell proliferation and protects from stress-induced cell death. *Exp. Cell Res.*, **314**, 738–747.

Leu, B., Koch, E. & Schmidt, J.T. (2010) GAP43 phosphorylation is critical for growth and branching of retinotectal arbors in zebrafish. *Dev. Neurobiol.*, **70**, 897–911.

Lieberoth, B.C., Becker, C.G. & Becker, T. (2003) Double labeling of neurons by retrograde axonal tracing and non-radioactive in situ hybridization in the CNS of adult zebrafish. *Methods Cell Sci.*, **25**, 65–70.

Lien, C.L., Schebesta, M., Makino, S., Weber, G.J. & Keating, M.T. (2006) Gene expression analysis of zebrafish heart regeneration. *PLoS Biol.*, **4**, e260.

Lilly, B., Clark, K.A., Yoshigi, M., Pronovost, S., Wu, M.L., Periasamy, M., Chi, M., Paul, R.J., Yet, S.F. & Beckerle, M.C. (2010) Loss of the serum response factor cofactor, cysteine-rich protein 1, attenuates neointima formation in the mouse. *Arterioscler. Thromb. Vasc. Biol.*, **30**, 694–701.

Liss, B., Haeckel, O., Wildmann, J., Miki, T., Seino, S. & Roeper, J. (2005) K-ATP channels promote the differential degeneration of dopaminergic midbrain neurons. *Nat. Neurosci.*, **8**, 1742–1751.

Louis, H.A., Pino, J.D., Schmeichel, K.L., Pomies, P. & Beckerle, M.C. (1997) Comparison of three members of the cysteine-rich protein family reveals functional conservation and divergent patterns of gene expression. *J. Biol. Chem.*, **272**, 27484–27491.

Ma, L., Yin, M., Wu, X., Wu, C., Yang, S., Sheng, J., Ni, H., Fukuda, M.N. & Zhou, J. (2006) Expression of trophinin and bystin identifies distinct cell types in the germinal zones of adult rat brain. *Eur. J. Neurosci.*, **23**, 2265–2276.

Ma, L., Greenwood, J.A. & Schachner, M. (2011) CRP1, a protein localized in filopodia of growth cones, is involved in dendritic growth. *J. Neurosci.*, **31**, 16781–16791.

Mattila, P.K. & Lappalainen, P. (2008) Filopodia: molecular architecture and cellular functions. *Nat. Rev. Mol. Cell Biol.*, **9**, 446–454.

McCurley, A.T. & Callard, G.V. (2010) Time course analysis of gene expression patterns in zebrafish eye during optic nerve regeneration. *J. Exp. Neurosci.*, **2010**, 17–33.

McLaughlin, C.R., Tao, Q. & Abood, M.E. (1994) Isolation and developmental expression of a rat cDNA encoding a cysteine-rich zinc finger protein. *Nucl. Acids Res.*, **22**, 5477–5483.

Minor, K., Tang, X., Kahrilas, G., Archibald, S.J., Davies, J.E. & Davies, S.J. (2008) Decorin promotes robust axon growth on inhibitory CSPGs and myelin via a direct effect on neurons. *Neurobiol. Dis.*, **32**, 88–95.

Miyasaka, K.Y., Kida, Y.S., Sato, T., Minami, M. & Ogura, T. (2007) Csrp1 regulates dynamic cell movements of the mesendoderm and cardiac mesoderm through interactions with Dishevelled and Diversin. *Proc. Natl. Acad. Sci. USA*, **104**, 11274–11279.

Morgenstern, D.A., Asher, R.A. & Fawcett, J.W. (2002) Chondroitin sulphate proteoglycans in the CNS injury response. *Prog. Brain Res.*, **137**, 313–332.

Pomies, P., Louis, H.A. & Beckerle, M.C. (1997) CRP1, a LIM domain protein implicated in muscle differentiation, interacts with alpha-actinin. *J. Cell Biol.*, **139**, 157–168.

Sadler, I., Crawford, A.W., Michelsen, J.W. & Beckerle, M.C. (1992) Zyxin and cCRP: two interactive LIM domain proteins associated with the cytoskeleton. *J. Cell Biol.*, **119**, 1573–1587.

Saul, K.E., Koke, J.R. & Garcia, D.M. (2010) Activating transcription factor 3 (ATF3) expression in the neural retina and optic nerve of zebrafish during optic nerve regeneration. *Comp. Biochem. Physiol. A Mol. Integr. Physiol.*, **155**, 172–182.

Schebesta, M., Lien, C.L., Engel, F.B. & Keating, M.T. (2006) Transcriptional profiling of caudal fin regeneration in zebrafish. *Sci. World J.*, **6** (Suppl 1), 38–54.

Schmeichel, K.L. & Beckerle, M.C. (1998) LIM domains of cysteine-rich protein 1 (CRP1) are essential for its zyxin-binding function. *Biochem. J.*, **331**, 885–892.

Schwab, M.E. & Bartholdi, D. (1996) Degeneration and regeneration of axons in the lesioned spinal cord. *Physiol. Rev.*, **76**, 319–370.

Seijffers, R., Allchorne, A.J. & Woolf, C.J. (2006) The transcription factor ATF-3 promotes neurite outgrowth. *Mol. Cell. Neurosci.*, **32**, 143–154.

Siebert, J.R., Middelton, F.A. & Stelzner, D.J. (2010) Intrinsic response of thoracic propriospinal neurons to axotomy. *BMC Neurosci.*, **11**, 69.

Silver, J. & Miller, J.H. (2004) Regeneration beyond the glial scar. *Nat. Rev. Neurosci.*, **5**, 146–156.

Skene, J.H. (1989) Axonal growth-associated proteins. *Annu. Rev. Neurosci.*, **12**, 127–156.

Tran, T.C., Singleton, C., Fraley, T.S. & Greenwood, J.A. (2005) Cysteine-rich protein 1 (CRP1) regulates actin filament bundling. *BMC Cell Biol.*, **6**, 45–57.

Vaillant, C., Meissirel, C., Mutin, M., Belin, M.F., Lund, L.R. & Thomasset, N. (2003) MMP-9 deficiency affects axonal outgrowth, migration, and apoptosis in the developing cerebellum. *Mol. Cell. Neurosci.*, **24**, 395–408.

Veldman, M.B., Bemben, M.A., Thompson, R.C. & Goldman, D. (2007) Gene expression analysis of zebrafish retinal ganglion cells during optic nerve regeneration identifies KLF6a and KLF7a as important regulators of axon regeneration. *Dev. Biol.*, **312**, 596–612.

Wullimann, M.F., Rupp, B. & Reichert, H. (1996) *Neuroanatomy of the Zebrafish Brain: A Topological Atlas*. Birkhauser, Basel.

Yiu, G. & He, Z. (2006) Glial inhibition of CNS axon regeneration. *Nat. Rev. Neurosci.*, **7**, 617–627.

Yu, Y.M., Cristofanilli, M., Valiveti, A., Ma, L., Yoo, M.S., Morellini, F. & Schachner, M. (2011a) The extracellular matrix glycoprotein tenascin-C promotes locomotor recovery after spinal cord injury in adult zebrafish. *Neuroscience*, **183**, 238–250.

Yu, Y.M., Gibbs, K.M., Davila, J., Campbell, N., Sung, S., Todorova, T.I., Otsuka, S., Sabaawy, H.E., Hart, R.P. & Schachner, M. (2011b) MicroRNA miR-133b is essential for functional recovery after spinal cord injury in adult zebrafish. *Eur. J. Neurosci.*, **33**, 1587–1597.

Zheng, B., Ho, C., Li, S., Keirstead, H., Steward, O. & Tessier-Lavigne, M. (2003) Lack of enhanced spinal regeneration in Nogo-deficient mice. *Neuron*, **38**, 213–224.